

# Ray Tracing Based Channel Analysis Involving Compact MIMO Antenna Arrays With Decoupling Networks

Mehmet Mert Taygur, Kun Wang, Thomas F. Eibert  
Chair of High-Frequency Engineering, Technical University of Munich  
Arcisstraße 21, 80333, Munich, Germany  
Email: mehmet.taygur@tum.de

**Abstract**—The channel characteristics of the compact Multiple Input Multiple Output (MIMO) antenna arrays with decoupling networks are studied. Two  $2 \times 2$  systems with monopole antennas are chosen as test cases. The analysis is performed by means of a ray tracing technique. Using such an asymptotic method allows to analyze large problems rather efficiently. This is especially critical for the outdoor propagation scenarios. The performances of different decoupling schemes under various propagation cases are investigated. After the channel coefficients have been obtained by the ray tracing simulation for a given scenario, the channel capacity can be calculated very easily using these coefficients. In order to have realistic channel representations, the losses arising from the decoupling networks are also considered during the simulations.

**Index Terms**—decoupling network, ray tracing, compact array, MIMO channel

## I. INTRODUCTION

Achieving higher channel capacity in wireless communications has always been one of the most fundamental problems. Multiple Input Multiple Output (MIMO) antenna systems are one way to accomplish this goal as they are superior to the conventional Single Input Single Output (SISO) systems. The literature on MIMO channel capacity is quite rich, albeit there are still many problems which are not thoroughly studied. Channel capacity analysis of the compact antenna arrays with decoupling networks is one of those problems whose applications might be essential for obtaining higher performance from diminished geometries.

The recent research about the MIMO performance analysis of the compact arrays mostly relies on matching and decoupling networks [1], although it has been shown that such a solution is not strictly necessary as it is possible to preserve the channel capacity by optimizing the array topology [2]. In this study, the traditional approach based on matching and coupling networks is used and two different decoupling schemes, namely, the eigenmode excitation and the multipoint conjugate matching [3] are investigated. The analysis is based on a ray tracing technique. By means of this asymptotic method, it is possible to analyze large problems, such as outdoor propagation scenarios, rather efficiently.

## II. ARRAYS WITH DECOUPLING NETWORK

Compact arrays, whose inter-element spacing is usually smaller than  $\lambda/2$ , suffer from significant mutual coupling that

consequently affects the power efficiency of the system. Due to restrictive geometric constraints of the problem, it may not be possible to increase the distance in order to avoid the problem. Nevertheless, it is possible to mitigate the issue by means of matching and decoupling techniques. In this study, two different schemes are employed; the eigenmode excitation and the conjugate matching. The actual array structure consists of two monopole antennas separated with  $0.1\lambda_0$  distance, where  $\lambda_0$  is the wavelength for the operating frequency (2.45 GHz). A picture of the array is given in Fig. 1.



Fig. 1. Two-element monopole array

### A. Eigenmode Excitation

Eigenmode analysis for the compact antenna arrays has been recently studied by Volmer *et al.* [4] and the measurements with a three element array indicate that it is possible to suppress the coupling coefficients way below -20 dB for a 100 MHz bandwidth, where the frequency was 1 GHz and the spacing between the elements was  $\lambda_0/4$ .

Consider an antenna array with  $m$  elements. Let  $\mathbf{S}$  be the scattering matrix, which is an  $m \times m$  symmetric matrix for the array. The eigenvalues of the scattering matrix  $\mathbf{S}$  can be found by solving

$$\det(\mathbf{S} - \Lambda \mathbf{I}) = 0, \quad (1)$$

where  $\mathbf{I}$  is a diagonal unit matrix. Then the relation between the eigenvalues and the eigenvectors can be expressed as

$$\mathbf{S} \mathbf{v}_i = \Lambda_i \mathbf{v}_i \quad i = 1, 2, \dots, m, \quad (2)$$

where  $\Lambda_i$  is the  $i$ th eigenvalue and  $\mathbf{v}_i$  is the eigenvector corresponding to that eigenvalue.

The main goal of the eigenmode decoupling is to excite the antenna array with an eigenvector of the scattering matrix  $\mathbf{S}$ . Thus, an additional decoupling network should be connected to the input port of the array. Let  $\mathbf{S}^D$  be the scattering matrix for this decoupling network having  $2m$  ports in total. Let us assume the network is reciprocal. Hence, it can be written

$$\mathbf{S}_{12}^D = (\mathbf{S}_{21}^D)^T. \quad (3)$$

Thus, the scattering matrix for the combined structure can be defined as

$$\mathbf{S}^C = \mathbf{S}_{11}^D + (\mathbf{S}_{21}^D)^T \mathbf{S} (\mathbf{I} - \mathbf{S}_{22}^D \mathbf{S})^{-1} \mathbf{S}_{21}^D. \quad (4)$$

In order to assure the decoupling, an eigenmode excitation through port  $i$  must not cause any reflection anywhere except from port  $i$ . Based on this criterion, solving (4) with an eigenmode excitation results into the conditions,

- 1) The network must be reciprocal.
- 2) The rows of  $\mathbf{S}_{21}^D$  must be eigenvectors  $v_i$  of  $\mathbf{S}$ .
- 3)  $\mathbf{S}_{22}^D$  must be either a zero matrix or have the same eigenvectors with  $\mathbf{S}$ .
- 4)  $\mathbf{S}_{11}^D$  must be diagonal, whose elements are solved by (4) where the expression equals zero.

According to the given design methodology, a simple network can be designed for generating the even and odd mode eigenvectors of the structure. In order to generate the odd mode, a  $180^\circ$  phase shifter is inserted near one of the ports. The array is mounted on a  $150 \text{ mm} \times 150 \text{ mm}$  aluminium plate and the network is realized on an FR4 substrate at the other side of the plate [3].

### B. Conjugate Matching

The conjugate matching works again with a network, which provides decoupling at the back-end. Let  $\mathbf{S}^D$  be the scattering matrix of this network. If the network is lossless and reciprocal, then it can be written

$$(\mathbf{S}^D)^H \mathbf{S}^D = \mathbf{I}, \quad (5)$$

where the operator  $(\ )^H$  denotes Hermitian transpose. Expansion into subblocks results into [5], [3]

$$\begin{aligned} (\mathbf{S}_{11}^D)^H \mathbf{S}_{11}^D + (\mathbf{S}_{21}^D)^H \mathbf{S}_{21}^D &= \mathbf{I} \\ (\mathbf{S}_{11}^D)^H \mathbf{S}_{12}^D + (\mathbf{S}_{21}^D)^H \mathbf{S}_{22}^D &= 0 \\ (\mathbf{S}_{12}^D)^H \mathbf{S}_{12}^D + (\mathbf{S}_{22}^D)^H \mathbf{S}_{22}^D &= \mathbf{I}, \end{aligned} \quad (6)$$

where the subscript 1 summarizes all accessible ports of the conjugate matching network and 2 summarizes all ports connected to the antenna array again described by its scattering matrix  $\mathbf{S}$ . If the maximum power criterion

$$(\mathbf{S})^H = \mathbf{S}_{22}^D, \quad (7)$$

is satisfied, decoupling can be achieved. Considering the coupling, the radiation behaviors and the symmetry of the

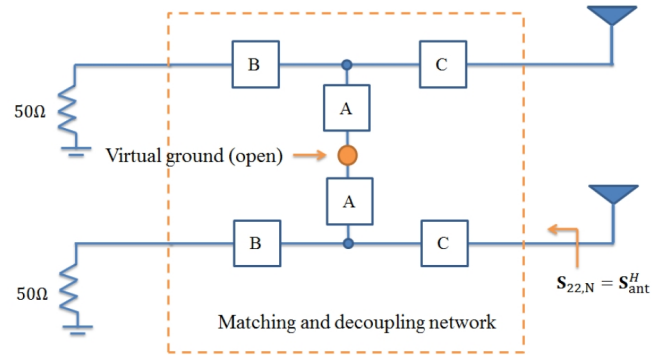


Fig. 2. Conjugate matching and decoupling network

structure, it can be said that the network would be an  $H$ -shaped structure, as shown in Fig. 2.

The main aim for synthesizing the given three network blocks  $A$ ,  $B$  and  $C$  is to make them lossless and symmetric. Using the even-odd mode excitation method, the networks are found to be:

$A$ : Two cascaded transmission lines having different characteristic impedances.

$B$ : Quarter wavelength transmission line to match  $50 \Omega$  line to the required admittance.

$C$ : Transmission line.

Similar to the eigenmode excitation structure, this array is also implemented on an aluminium plate with the same dimensions and FR4 substrate at the back [3].

### III. MIMO CHANNEL CAPACITY

For a given MIMO system with the channel matrix  $\mathbf{H}$ , the transmitting signal vector  $\mathbf{x}$  and the noise vector  $\mathbf{n}$ , the received signal vector  $\mathbf{y}$  can be expressed as

$$\mathbf{y} = \mathbf{H}\mathbf{x} + \mathbf{n}. \quad (8)$$

Then, the channel capacity is obtained as [6]

$$C = \log_2 \left( \det \left( \mathbf{I} + \rho \mathbf{H} \mathbf{Q} (\mathbf{H})^H \right) \right), \quad (9)$$

where  $\mathbf{Q}$  is the covariance matrix for the transmitted signal and  $\rho$  is the average signal to noise ratio (SNR). If the channel matrix is known, then the capacity can be calculated by using (9). The individual elements of the channel matrix will be determined by the ray tracing simulations together with the particular compact antenna array properties in this work. The individual matrix elements are obtained by the ratio of the generator voltage at the transmitter to the load voltage at the receiver. Such a choice would reveal all the environmental effects as well as the antenna imperfections, like efficiency.

### IV. RAY TRACING

Ray tracing is a simulation method which is generally used for solving electromagnetic problems, where the wavelength is small compared to the problem geometry. Solving such problems with the integral/differential equation based methods,

like the finite element method (FEM), the method of moments (MoM), may require huge computational resources and time. Using an asymptotic technique, such as Geometrical Optics (GO), Uniform Theory of Diffraction (UTD), mitigates these requirements greatly, without sacrificing the accuracy very much. First introduced by Deschamps [7], ray tracing has become a widespread method for solving electrically large problems as the computers have become more powerful over the years.

The ray tracing tool, which is used for this study, has been developed by the Technical University of Munich and AUDI AG [8]. The workflow of the ray tracer can be summarized as

- 1) The problem geometry is created with any 3D modelling software, then converted to .osg format.
- 2) The simulation configuration parameters are defined in an .xml file. The transmitters and the receivers are implemented with their respective radiation patterns in this file as well.
- 3) The program reads the geometry and the configuration files, then initiates the ray launching engine, which is based on the NVIDIA OptiX framework [9].
- 4) By means of the OptiX framework, rays are launched from the transmitters, traced throughout the geometry while the interactions are determined (reflection, refraction, diffraction etc.) according to the given material configurations. The path of each ray is traced until either the ray hits a receiver sphere or, a maximum number of interactions (a predetermined value defined in configuration) is reached or the ray leaves the scene.
- 5) Once the paths of the rays have been determined, the electromagnetic fields are calculated according to the GO/UTD principles.

It should be noted that NVIDIA OptiX is a GPU based framework, where the graphics card is used as the computing element. Therefore, all the operations related with ray tracing are performed in the GPU with massive parallelism. The EM field calculations are not handled by the OptiX though it is done on the GPU as well, by means of the Thrust library. These two processes are the main elements of the ray tracer tool. Since both procedures are handled in the GPU, the solution time can be as low as a few seconds for the relevant problems.

### A. Ray Tracing

The ray tracing process traces the rays in the geometry according to the material properties and the geometrical configuration of the surrounding environment. Each ray is first launched from a transmitter with a certain direction. The OptiX framework then detects whether any object is hit and if it is, which kind of interaction must occur. There are 6 different events which a ray experiences after the launch. These are:

- 1) Receiver Hit: Ray hits the receiver sphere.
- 2) Miss: Ray leaves the geometry without hitting any receiver.
- 3) Reflection.
- 4) Refraction.

- 5) Diffusion.
- 6) Diffraction.

A ray is traced until a Receiver Hit or Miss occurs, or a predefined maximum number of interactions is achieved. A flowchart for the ray tracing process is given in Fig. 3.

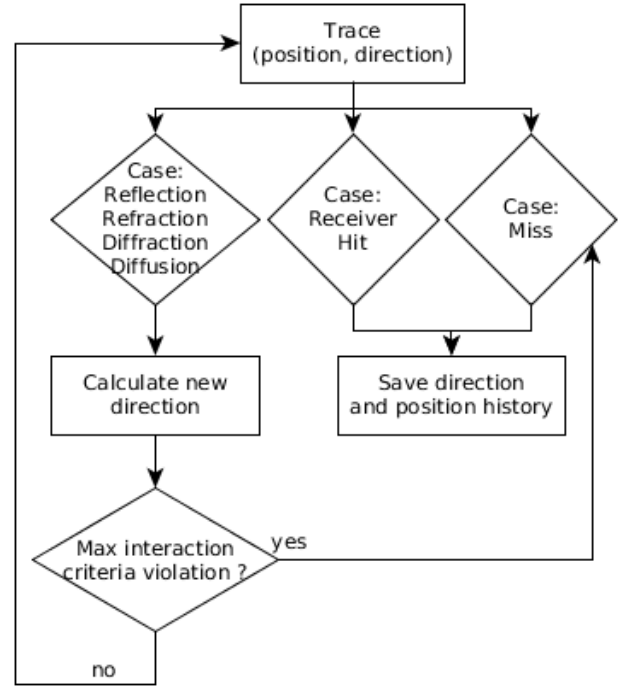


Fig. 3. Path tracing flowchart

After the ray tracing process is complete, a typical scenario might consist of millions of ray data. This data must be filtered for further processing. Since most of these would be Miss rays already, the initial set is significantly reduced. All remaining data consist of Receiver Hit rays. The elimination criteria are based on the history of each ray, which is basically the ray-object interaction history. Two rays, which interacted with the same objects throughout the geometry, are considered equal. Among those, the one which is closest to the receiver center, is kept.

### B. Field Calculations

Field calculations are based on the individual history of a ray. Each ray had already assigned 4 different events for material interactions at certain points. The field calculations at these interaction points are calculated according to:

- 1) Reflection: Fresnel coefficients.
- 2) Refraction: Fresnel coefficients.
- 3) Diffraction: Uniform Theory of Diffraction.
- 4) Diffusion: Lambert Reflectance.

Between these interaction points, a ray is simply considered to propagate in the environment.

## V. SIMULATIONS

One outdoor and one indoor scenario are used for channel capacity analysis. The simulations are performed with multiple receivers at different positions and a single transmitter at a fixed position. Both cases are designed to simulate NLOS propagation. It can be predicted that the channel coefficients would be very low since the distances might easily exceed couple hundred wavelengths even for indoor scenario. Additionally, the interactions with the surrounding geometry will cause attenuation.

### A. Outdoor Scenario

A simple outdoor propagation scenario is created for the ray tracer simulation in order to evaluate the channel capacity. The scenario is inspired from a basic urban scenery. There are 9 building blocks, each having a  $20 \times 20 \text{ m}^2$  ground area but with different heights. The buildings are located such that a  $3 \times 3$  grid is formed with 10 m distance among each block. The entire structure covers a  $100 \times 100 \text{ m}^2$  area. The channel analysis is performed for 5 different receiver locations ( $x = 35 \text{ m}, 25 \text{ m}, 15 \text{ m}, 5 \text{ m}, -5 \text{ m}$ ,  $y = 15 \text{ m}$ ) while the transmitter position was fixed ( $x = -30 \text{ m}$ ,  $y = -15 \text{ m}$ ). An illustration of the scenario is given in Fig. 4.

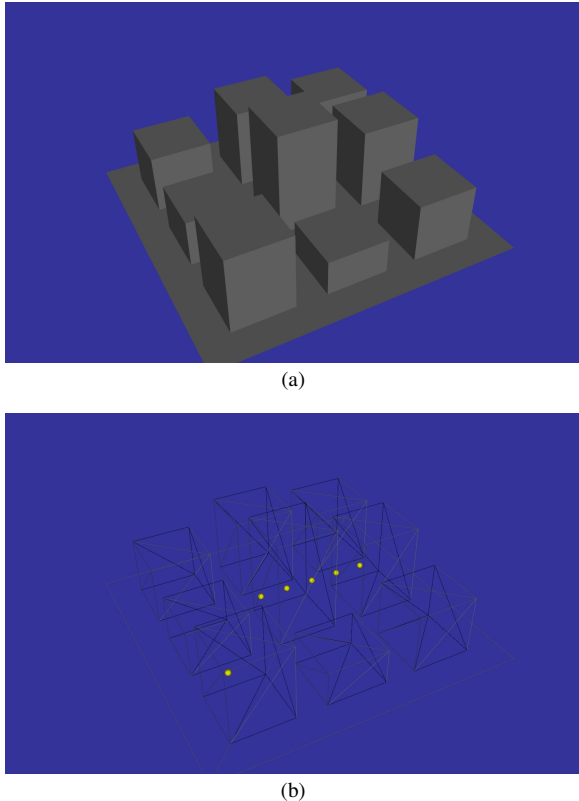


Fig. 4. Scenario illustration with (a) solid objects (b) mesh structure and receiver-transmitter locations

It should be noted that the simulations for each receiver position are performed separately. The receiver positions are all shown in a single figure due to convenience. The ray tracing has been performed with 10 million launches. Only reflection

phenomena were taken into account and the maximum number of interactions was limited to 10. All the objects in the geometry were assumed as concrete. Therefore, they have the same dielectric constant,  $\epsilon_r = 5 - j0.1 \text{ F/m}$ . The operating frequency was 2.45 GHz. The ray paths are shown in Fig. 5.

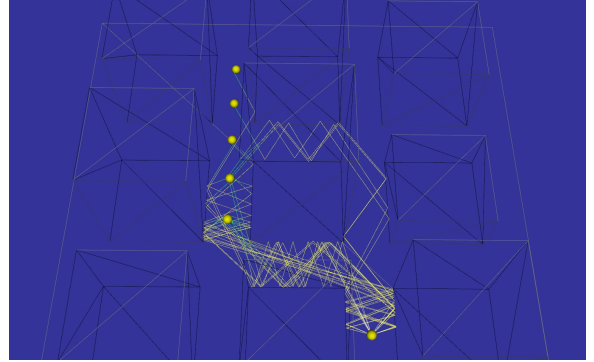


Fig. 5. Ray paths between transmitter and receivers

As the receiver comes close to the transmitter, alternative paths, which reach the receiver (the green line segments), appear. This yields increased diversity. A MIMO channel capacity computation has been performed with  $\rho = 30 \text{ dB}$  without any channel state information neither at the receiver nor at the transmitter side. With uniform power distribution among the transmit channels, this results into

$$\mathbf{Q} = \frac{\mathbf{I}}{N_t}, \quad (10)$$

where  $N_t$  is the number of the transmitting antennas. The obtained channel capacities are shown in Fig. 6.

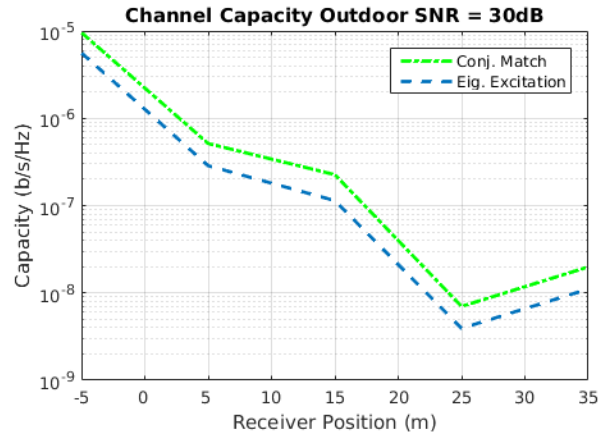


Fig. 6. Outdoor channel capacity dependent on the receiver position

### B. Indoor Scenario

A similar capacity analysis is made with a different geometry, where a transmitter outside of a house-like structure and 6 different receivers exist in two separate rooms. An illustration of the scenario is given in Fig. 7.

Different from the previous case, the indoor scenario includes metal (PEC) and wood ( $\epsilon_r = 2.7 - j0.3 \text{ F/m}$ ) as

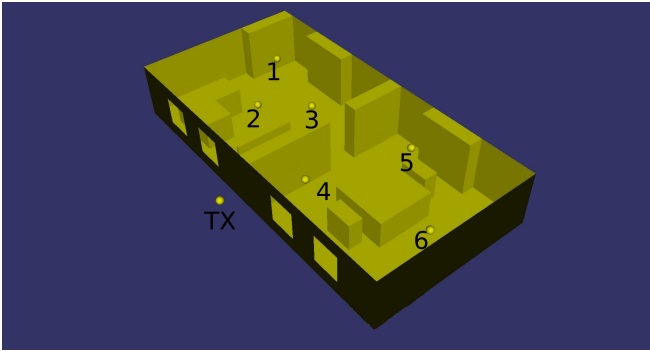


Fig. 7. Indoor channel capacity for different receivers

additional materials. The transmitter is placed to satisfy NLOS propagation for each receiver. The capacity calculation results are given in Fig. 8.

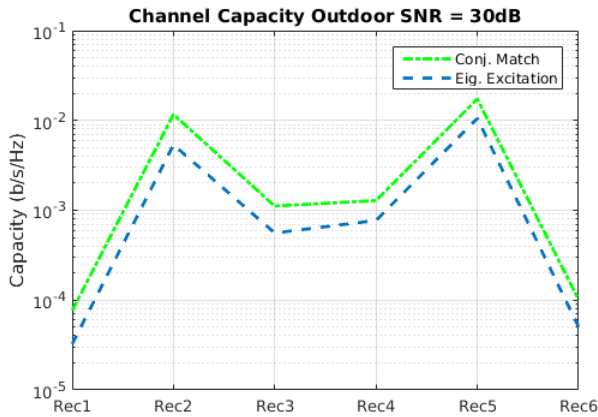


Fig. 8. Indoor channel capacity for different receivers

Both results indicate that the conjugate matched array pair is superior compared to the eigenmode excitation. This can be explained with the difference between the angular diversities of the patterns and the losses in the antennas.

## VI. CONCLUSIONS

A novel and innovative graphics card based ray tracing simulator has been utilized to investigate the channel capacities of multiple antenna systems with closely spaced but decoupled antenna elements. The particular antenna properties, such as the losses in the antennas and in the decoupling networks as well as the antenna element radiation patterns, have been carefully considered in the simulations. It was found that the multiple antenna performance depends strongly on the propagation scenario and also on the specific antenna properties, which should be carefully considered in the antenna design and realization.

## REFERENCES

[1] R.A. Bhatti, S. Yi, and S. Park, "Compact Antenna Array With Port Decoupling for LTE-Standardized Mobile Phones", *IEEE Antennas And Wireless Propagation Letters*, vol. 8, pp. 1430-1433, 2009

[2] D.W. Browne, M. Manteghi, M.P. Fitz, and Y. Rahmat-Samii, "Experiments With Compact Antenna Arrays for MIMO Radio Communications", *IEEE Transactions on Antennas and Propagation*, vol. 54, no. 11, pp. 3239-3250, 2006

[3] K. Wang, L. Li, and T.F. Eibert, "Comparison of Compact Monopole Antenna Arrays With Eigenmode Excitation and Multiport Conjugate Matching", *IEEE Transactions on Antennas and Propagation*, vol. 61, no. 8, pp. 4054-4062, 2013

[4] C. Volmer, J. Weber, R. Stephan, K. Blau, and M.A. Hein, "An Eigen-Analysis of Compact Antenna Arrays and Its Application to Port Decoupling", *IEEE Transactions Antennas and Propagation*, vol. 56, no. 2, pp. 360-370, 2008

[5] J.W. Wallace, and M.A. Jensen, "Termination-Dependent Diversity Performance of Coupled Antennas: Network Theory Analysis", *IEEE Transactions On Antennas And Propagation*, vol. 52, no. 1, pp. 98-105, 2004

[6] E. Telatar, "Capacity of Multi-Antenna Gaussian Channels", *European Transactions on Telecommunications*, vol. 10, no. 6, pp. 585-595, 1999

[7] G.A. Deschamps, "Ray Techniques in Electromagnetics", *Proceedings of the IEEE*, vol. 60, no. 9, pp. 1022-1035, 1972

[8] M. Mocker, M. Schiller, R. Brem, Z. Sun, H. Tazi, T.F. Eibert, and A. Knoll, "Combination of A Full-Wave Method and Ray Tracing For Radiation Pattern Simulations of Antennas on Vehicle Roofs", *European Conference on Antennas and Propagation*, Lisbon, 2015

[9] S.G. Parker, J. Bigler, A. Dietrich, H. Friedrich, J. Hoberock, D. Lbke, D. McAllister, M. McGuire, K. Morley, A. Robison, and M. Stich, "OptiX: A General Purpose Ray Tracing Engine", (Online) <http://graphics.cs.williams.edu/papers/OptiXSIGGRAPH10/Parker10OptiX.pdf>